

## Application of Halpin-Tsai Method in Modelling and Size-dependent Vibration Analysis of CNTs/fiber/polymer Composite Microplates

Ghorbanpour Arani<sup>1,2†</sup>, H. Baba Akbar Zarei<sup>2</sup>, E. Haghparast<sup>2</sup>

<sup>1</sup>Faculty of Mechanical Engineering, University of Kashan, Kashan, Iran  
<sup>2</sup>Institute of Nanoscience & Nanotechnology, University of Kashan, Kashan, Iran

Received: 26 Jan 2016 , Accepted: 4 Apr. 2016

### Abstract

In the present study, modelling and vibration analysis of Carbon nanotubes/ fiber/ polymer composite microplates are investigated. The governing equations of the Carbon nanotubes/ fiber/ polymer composite microplates are derived based on first order shear deformation plate theory, rather than other plate theories, due to accuracy and simplicity of polynomial functions. The modified couple stress theory is employed because of its capability to interpret the size effect. Halpin-Tsai model is utilized to evaluate the material properties of two-phase composite consisted of uniformly distributed and randomly oriented Carbon nanotubes through the epoxy resin matrix. Afterwards, the structural properties of carbon nanotubes reinforced polymer matrix, which is assumed as a new matrix, and then, reinforced with E-Glass fiber, they are calculated by fiber micromechanics approach. Employing Hamilton's principle, the equations of motion are obtained and solved by Hybrid analytical numerical method. The influences of various parameters such as the weight percentage of single-walled carbon nanotube, aspect ratio, and size effect on the vibration characteristics of microplate are discussed in details. Results indicate that the stability of Carbon nanotubes/fiber/polymer composite microplates can be improved by adding appropriate values of Carbon nanotubes. In addition, increase in the frequencies is more pronounced in the case of microplates reinforced with SWCNT compared with MWCNT. These findings can be used in design and manufacturing of marine vessels and aircrafts.

### Keywords:

*Halpin-Tsai model, modified couple stress theory, multiscale composite plate, vibration analysis*

### 1. Introduction

Carbon nanotubes (CNTs) are molecular structures of

graphitic carbons with excellent and remarkable properties. The exceptional mechanical properties of

---

† Tel.: +98 31 55912450; Fax: +98 31 55912424.  
E-mail address: aghorban@kashanu.ac.ir

the CNTs, combined with their low density, offer scope for the development of nanotube reinforced composite materials. Due to their extraordinary specific stiffness and strength, the study of micro- and nano-composites reinforced with CNTs represent tremendous opportunity for researchers and industrialists. Therefore, the presence of the CNTs can improve the strength and stiffness of structures as well as electrical and thermal conductivities to composite systems.

In micro- and nano-scale studies, it is important to consider the size effect. Due to lack of material length scale parameters, conventional plate models based on classical continuum theories do not consider the size effects, while the size effects have been observed [1-3] experimentally. Therefore, size-dependent plate models based on size-dependent continuum theories that contain additional material length scale parameters have been developed. Several size-dependent continuum theories have been developed to account for the size effects, such as the classical couple stress theory (CCST) [4] and the nonlocal elasticity theory [5] with two material length scale parameters, and the strain gradient theory (SGT) [6] with three material length scale parameters. Considering the difficulties in determining material length scale parameters, the modified couple stress theory (MCST) [7] takes an advantage over the aforementioned size-dependent continuum theories containing only one material length scale parameter. Also, MCST includes asymmetric couple stress tensor respect to CCST.

Tsiatas's investigation [8] can be noted as one of the first works that employed modified couple stress theory (MCST) for plate. He developed a Kirchhoff plate model based on a MCST for static analysis of microplates. Then, Yin et al. [9] and Jomehzadeh et al. [10] utilized this model to study the vibration of microplates. Asghari [11] studied geometrically nonlinear micro-plate formulation with Kirchhoff plate theory of isotropic plates. He presents the general form of boundary conditions considering the sharp corners. Also, Sahmani and Ansari [12] presented SGT for the free vibration of functionally graded (FG) micro-plates based on non-classical higher-order shear deformable plate model and Mori-Tanaka homogenization technique. They obtained that in the higher length scale parameters, the material property gradient index has more effects on the vibration behavior of FG micro plates for MCST and strain gradient theory (SGT) with respect to classical plate theory (CPT). Mohammadimehr et al. [13] presented the size-dependent effect on the buckling and vibration analysis of double-bonded nanocomposite piezoelectric plate reinforced by boron nitride nanotube. Using MCST, they studied the effects of material length scale

parameter, elastic foundation coefficients, and transverse and longitudinal wave numbers, etc. on the dimensionless natural frequency.

Motivated by the aforementioned ideas, the vibration analysis of CNTs/ fiber/ polymer multiscale composite microplate is investigated in this study for the first time. Halpin-Tsai model and fiber micromechanics approach are used to determine the material properties of the multiscale composite plate. Also, first order shear deformation plate theory (FSDT) is selected for the displacement field. To consider the size effects, MCST are utilized to obtain strain energy. Finally, the equations of motion for microplate are derived based on Hamilton's principle and solved by means of hybrid analytical numerical method for simply supported boundary conditions. Effects of various parameters such as the weight percentage of single-walled carbon nanotube, aspect ratio, and size effect on the dimensionless frequencies of microplates are investigated. The natural frequencies of plates are compared with the previous studies in literature to verify the presented research. The result of this work can be useful to control and improve the performance of composite devices which are employed in military equipment's.

## 2. Micromechanics modelling

Consider a multiscale composite microplate composed of matrix ( $m$ ) and fiber ( $f$ ) phases. Note that matrix phase consists of CNTs and resin where CNTs were assumed to be uniformly distributed and randomly oriented through the matrix. To predict the material properties of multiscale composite, a combination of Halpin-Tsai model and micromechanics approach were used in hierarchy as shown in Figure 1.

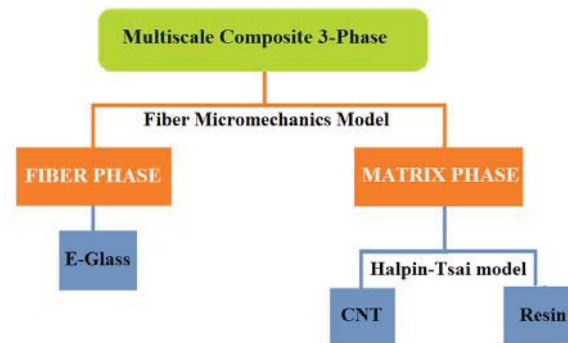


Fig. 1. A hierarchical configuration for modelling of three phase multiscale composite

### 2.1. Halpin-Tsai model

The elastic properties of matrix phase can be calculated by a semi-empirical method. According to Halpin-Tsai model, the tensile modulus of matrix phase

can be expressed as [14, 15]:

$$E^m = \left[ \frac{3}{8} \left( 1 + 2 \frac{l_{NT} \eta_L V_{NT}}{d_{NT}} \right) (1 - \eta_L V_{NT})^{-1} + \frac{5}{8} \frac{2\eta_D V_{NT} + 1}{1 - \eta_D V_{NT}} \right] E_{epoxy}, \quad (1a)$$

$$\eta_L = \left[ \left( \frac{E_{NT}}{E_{epoxy}} \right) - \left( \frac{d_{NT}}{4t} \right) \right] \left[ \left( \frac{E_{NT}}{E_{epoxy}} \right) + \left( \frac{l_{NT}}{2t} \right) \right]^{-1} \quad (1b)$$

$$\eta_D = \left[ \left( \frac{E_{NT}}{E_{epoxy}} \right) - \left( \frac{d_{NT}}{4t} \right) \right] \left[ \left( \frac{E_{NT}}{E_{epoxy}} \right) + \left( \frac{d_{NT}}{2t} \right) \right] \quad (1c)$$

$$V_{NT} = \frac{w_{NT}}{w_{NT} + (\rho_{NT} / \rho_{epoxy}) - (\rho_{NT} / \rho_{epoxy})} \quad (1d)$$

where  $E$ ,  $V$ ,  $w$ , and  $\rho$  represent Young's modulus, volume fraction, mass fraction, and density, respectively. Also,  $d_{NT}$ ,  $l_{NT}$ , and  $t$  are diameter, length, and thickness of CNT, respectively. Hence, the subscripts  $NT$  and  $epoxy$  are related to CNT and the resin epoxy, respectively. Therefore, the shear modulus of matrix phase can be calculated by:

$$G^m = \frac{E^m}{2(1 + \nu^m)}, \quad (2a)$$

$$\nu_{12}^m = \nu_{epoxy}, \quad (2b)$$

in which,  $\nu$  is Poisson ratio.

## 2.2. Micromechanics approach

The elastic properties of the microplate can be determined by Micromechanics approach as follows [16]:

$$E_{11} = E_{11}^f V^f + E^m V^m, \quad (3a)$$

$$\frac{1}{E_{22}} = \frac{V^f}{E_{22}^f} + \frac{V^m}{E^m} - V^f V^m \left( \frac{(\nu^f)^2 E^m / E_{22}^f + (\nu^m)^2 E_{22}^f / E^m - 2\nu^f \nu^m}{\nu^f E_{22}^f + \nu^m E^m} \right), \quad (3b)$$

$$\frac{1}{G_{12}} = \frac{V^f}{G_{12}^f} + \frac{V^m}{G^m}, \quad (3c)$$

$$\rho^c = \rho^f V^f + \rho^m V^m, \quad (3d)$$

$$\nu_{12} = \nu_{12}^f V^f + \nu^m V^m, \quad (3e)$$

where  $E_{11}$  and  $E_{22}$  are longitudinal and transverse

Young's modulus, respectively. Also,  $G_{12}$  is in plane shear modulus.

## 3. Fundamental relations

As shown in Figure 2, consider rectangular microplate with length  $a$ , width  $b$ , and thickness  $h$ . The global coordinate system ( $x$ ,  $y$ , and  $z$  axis) is located in mid-plane so that the origin is at one corner of microplate. According to FSDT, displacement field of microplate can be expressed as follows [17]:

$$\begin{aligned} U(x, y, z, t) &= u(x, y, t) - z \frac{\partial w(x, y, t)}{\partial x} + z \phi_x(x, y, t), \\ V(x, y, z, t) &= v(x, y, t) - z \frac{\partial w(x, y, t)}{\partial y} + z \phi_y(x, y, t), \end{aligned} \quad (4)$$

$$W(x, y, z, t) = w(x, y, t),$$

in which,  $u$ ,  $v$ , and  $w$  represent displacement through the  $x$ ,  $y$ , and  $z$  axes, respectively. Also,  $\phi_x$  and  $\phi_y$  are the rotational about  $x$  and  $y$  axes, respectively.

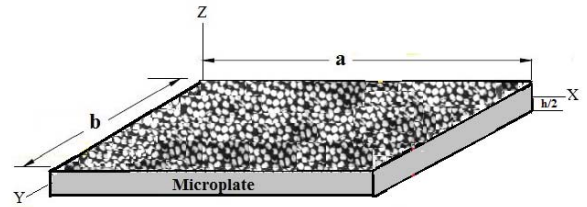


Fig. 2. Schematic figure of CNTs/fiber/polymer multiscale composite microplate

The linear strain relations can be described as:

$$\begin{Bmatrix} \varepsilon_{xx} \\ \varepsilon_{yy} \\ \gamma_{xy} \end{Bmatrix} = \begin{Bmatrix} \frac{\partial u}{\partial x} \\ \frac{\partial v}{\partial y} \\ \frac{\partial u}{\partial y} + \frac{\partial v}{\partial x} \end{Bmatrix} + z \begin{Bmatrix} -\frac{\partial^2 w}{\partial x^2} + \frac{\partial \phi_x}{\partial x} \\ -\frac{\partial^2 w}{\partial y^2} + \frac{\partial \phi_y}{\partial y} \\ -2\frac{\partial^2 w}{\partial x \partial y} + \frac{\partial \phi_x}{\partial y} + \frac{\partial \phi_y}{\partial x} \end{Bmatrix}, \quad \begin{Bmatrix} \gamma_{xz} \\ \gamma_{yz} \end{Bmatrix} = k_s \begin{Bmatrix} \phi_x \\ \phi_y \end{Bmatrix} \quad (5)$$

in which,  $\varepsilon$  and  $\gamma$  are normal strains and shear strains, respectively, and  $k_s$  is shear correction factor. It should be noted that  $\varepsilon_{zz} = 0$ . Based on the Hook's law, the constitutive equations can be expressed as:

$$\begin{Bmatrix} \sigma_{xx} \\ \sigma_{yy} \\ \sigma_{xy} \\ \sigma_{yz} \\ \sigma_{xz} \end{Bmatrix} = \begin{bmatrix} Q_{11} & Q_{12} & 0 & 0 & 0 \\ Q_{12} & Q_{22} & 0 & 0 & 0 \\ 0 & 0 & Q_{66} & 0 & 0 \\ 0 & 0 & 0 & Q_{44} & 0 \\ 0 & 0 & 0 & 0 & Q_{55} \end{bmatrix} \begin{Bmatrix} \varepsilon_{xx} \\ \varepsilon_{yy} \\ \gamma_{xy} \\ \gamma_{yz} \\ \gamma_{xz} \end{Bmatrix}, \quad (6)$$

where

$$\begin{aligned} Q_{11} &= \frac{E_{11}}{1-\nu_{12}\nu_{21}}, \quad Q_{12} = \frac{\nu_{12}E_{11}}{1-\nu_{12}\nu_{21}}, \\ Q_{21} &= \frac{\nu_{21}E_{11}}{1-\nu_{12}\nu_{21}}, \quad Q_{22} = \frac{E_{22}}{1-\nu_{12}\nu_{21}} \\ Q_{44} &= G_{23}, \quad Q_{66} = G_{12}, \quad Q_{55} = G_{13}, \end{aligned} \quad (7)$$

$\sigma_{pq}$  ( $p, q = x, y, z$ ) are stresses and  $Q_{rs}$  ( $r, s = 1, 2$  and 44, 55, 66) are the material constants. Microplate is made of single orthotropic layer while reinforced by fibers. 1, 2, 6, 4, and 5 denote the local coordinate axes where 1 axis is along fibers direction, 2 axis is normal to fibers direction, and 6 axis is shown shear in-plane direction. Also, 4 and 5 represent shear out of plain directions. Therefore, the constitutive equations must be transformed to the global coordinates. So, the constitutive equations of multiscale composite can be rewritten as follows [16].

$$\begin{Bmatrix} \sigma_{xx} \\ \sigma_{yy} \\ \sigma_{xy} \\ \sigma_{yz} \\ \sigma_{xz} \end{Bmatrix} = \begin{bmatrix} \overline{Q}_{11} & \overline{Q}_{12} & \overline{Q}_{16} & 0 & 0 \\ \overline{Q}_{12} & \overline{Q}_{22} & \overline{Q}_{26} & 0 & 0 \\ \overline{Q}_{16} & \overline{Q}_{26} & \overline{Q}_{66} & 0 & 0 \\ 0 & 0 & 0 & \overline{Q}_{44} & \overline{Q}_{45} \\ 0 & 0 & 0 & \overline{Q}_{45} & \overline{Q}_{55} \end{bmatrix} \begin{Bmatrix} \varepsilon_{xx} \\ \varepsilon_{yy} \\ \gamma_{xy} \\ \gamma_{yz} \\ \gamma_{xz} \end{Bmatrix}, \quad (8)$$

where  $\overline{Q}_{ij}$  ( $i, j = 1, 2, 6$  and 4, 5) are given as:

$$\begin{aligned} \overline{Q}_{11} &= m^4 Q_{11} + n^4 Q_{22} + 2m^2 n^2 Q_{12} + 4m^2 n^2 Q_{66}, \\ \overline{Q}_{22} &= n^4 Q_{11} + m^4 Q_{22} + 2m^2 n^2 Q_{12} + 4m^2 n^2 Q_{66}, \\ \overline{Q}_{12} &= m^2 n^2 Q_{11} + m^2 n^2 Q_{22} + (m^4 + n^4) Q_{12} - 4m^2 n^2 Q_{66}, \\ \overline{Q}_{16} &= m^3 n Q_{11} + mn^3 Q_{22} + (mn^3 - m^3 n) Q_{12} + 2(mn^3 - m^3 n) Q_{66}, \\ \overline{Q}_{26} &= mn^3 Q_{11} + m^3 n Q_{22} + (m^3 n - mn^3) Q_{12} + 2(m^3 n - mn^3) Q_{66}, \\ \overline{Q}_{66} &= m^2 n^2 Q_{11} + m^2 n^2 Q_{22} - 2m^2 n^2 Q_{12} + (m^2 - n^2)^2 Q_{66}, \\ \overline{Q}_{44} &= m^2 Q_{44} + n^2 Q_{55}, \quad \overline{Q}_{45} = mn(Q_{55} - Q_{44}), \\ \overline{Q}_{55} &= n^2 Q_{44} + m^2 Q_{55}, \end{aligned} \quad (9)$$

in which,  $m = \cos\phi$  and  $n = \sin\phi$  ( $\phi$  being the angle between global  $x$  axis and fiber axes).

#### 4. Hamilton's principle

Hamilton's principle is employed to derive the motion equations as follows [18]:

$$\delta \Pi = \delta \int_{t_1}^{t_2} (U_s - K) dt = 0, \quad (10)$$

in which,  $U_s$  and  $K$  represent strain energy and kinetic energy, respectively. MCST is used to derive equations of strain energy as [17]:

$$U_s = \frac{1}{2V} \int \left( \sigma_{xx} \varepsilon_{xx} + \sigma_{yy} \varepsilon_{yy} + \sigma_{zz} \varepsilon_{zz} + \sigma_{xy} \gamma_{xy} + \sigma_{xz} \gamma_{xz} + \sigma_{yz} \gamma_{yz} \right) dV + \quad (11)$$

$$\frac{1}{2V} \int \left( m_{xx} \chi_{xx} + m_{yy} \chi_{yy} + m_{zz} \chi_{zz} + m_{xy} \chi_{xy} + m_{xz} \chi_{xz} + m_{yz} \chi_{yz} \right) dV,$$

$\chi_{pq}$  is symmetric curvature tensor and  $m_{pq}$  is deviatoric part of the couple stress tensor. Also,  $m_{pq}$  is the stress which is palpable in the small scale and cannot be ignored and is defined as:

$$m_{pq} = M \chi_{pq}, \quad (12a)$$

$$M = 2l_0^2 G, \quad (12b)$$

$$\chi_{pq} = \frac{1}{2} \left( e_{pij} \frac{\partial \varepsilon_{jq}}{\partial x_i} + e_{qij} \frac{\partial \varepsilon_{jp}}{\partial x_i} \right), \quad (12c)$$

where  $l_0$  and  $e_{pij}$  represent the material length scale parameter and alternate tensor, respectively. Also,  $G$  is equal to  $\overline{Q}_{66}$  in this paper. So, the symmetric curvature tensor can be rewritten by substituting Eq. (5) into Eq. (12c) as follows:

$$\chi_{xx} = \frac{\partial^2 w}{\partial y \partial x} - \frac{1}{2} \frac{\partial \phi_y}{\partial x}, \quad (13a)$$

$$\chi_{yy} = -\frac{\partial^2 w}{\partial y \partial x} + \frac{1}{2} \frac{\partial \phi_x}{\partial y}, \quad (13b)$$

$$\chi_{zz} = \frac{1}{2} \left( \frac{\partial \phi_y}{\partial x} - \frac{\partial \phi_x}{\partial y} \right), \quad (13c)$$

$$\chi_{xy} = \frac{1}{4} \left( \frac{\partial \phi_x}{\partial x} - \frac{\partial \phi_y}{\partial y} \right) + \frac{1}{2} \left( \frac{\partial^2 w}{\partial y^2} - \frac{\partial^2 w}{\partial x^2} \right), \quad (13d)$$

$$\chi_{xz} = \frac{1}{4} \left( \frac{\partial^2 v}{\partial x^2} - \frac{\partial^2 u}{\partial y \partial x} \right) + \frac{1}{4} z \left( \frac{\partial^2 \phi_y}{\partial x^2} - \frac{\partial^2 \phi_x}{\partial y \partial x} \right), \quad (13e)$$

$$\chi_{yz} = \frac{1}{4} \left( \frac{\partial^2 v}{\partial y \partial x} - \frac{\partial^2 u}{\partial y^2} \right) + \frac{1}{4} z \left( \frac{\partial^2 \phi_y}{\partial y \partial x} - \frac{\partial^2 \phi_x}{\partial y^2} \right). \quad (13f)$$

Substituting Eq. (5) into Eq. (8) and using Eqs. (11)-(13), strain energy can be obtained. Also, the kinetic energy of microplate can be determined by:

$$K = \frac{1}{2V} \int \rho^c \left( \left( \frac{\partial u}{\partial t} \right)^2 + \left( \frac{\partial v}{\partial t} \right)^2 + \left( \frac{\partial w}{\partial t} \right)^2 \right) dV. \quad (14)$$

Substituting Eq. (4) into Eq. (14), kinetic energy can be calculated. Now, using Hamilton's principle and putting the coefficients of  $\delta u$ ,  $\delta v$ ,  $\delta w$ ,  $\delta \phi_x$ , and  $\delta \phi_y$  equal to zero, the motion equations are obtained. For the sake of brevity, these equations are not

presented here.

### 5. Solution Procedure

In the case of simply supported microplate, the displacement components can be defined according to the Navier’s procedure, which automatically satisfy the boundary conditions at the microplate edges. Based on this procedure, the displacement components can be expressed in the following forms:

$$\begin{aligned}
 u(x, y, t) &= \sum_m \sum_n U_{mn} \cos(\alpha x) \sin(\beta y) e^{i \omega_{mn} t}, \\
 v(x, y, t) &= \sum_m \sum_n V_{mn} \cos(\beta y) \sin(\alpha x) e^{i \omega_{mn} t}, \\
 w(x, y, t) &= \sum_m \sum_n W_{mn} \sin(\alpha x) \sin(\beta y) e^{i \omega_{mn} t}, \\
 \phi_x(x, y, t) &= \sum_m \sum_n P_{mn} \cos(\alpha x) \sin(\beta y) e^{i \omega_{mn} t}, \\
 \phi_y(x, y, t) &= \sum_m \sum_n Q_{mn} \cos(\beta y) \sin(\alpha x) e^{i \omega_{mn} t},
 \end{aligned} \tag{15}$$

in which,  $i = \sqrt{-1}$ ,  $\alpha = \frac{m\pi}{a}$ , and  $\beta = \frac{n\pi}{b}$ .  $m$  and  $n$  show the wave or mode numbers along the  $x$  and  $y$  directions, respectively. Also,  $U_{mn}$ ,  $V_{mn}$ ,  $W_{mn}$ ,  $P_{mn}$ , and  $Q_{mn}$  are unknown coefficients of each mode

numbers and  $\omega_{mn}$  denotes the natural frequency. Inserting the displacement components from Eq. (15) into the motion equations, final relation is obtained as a matrix form:

$$\underbrace{\begin{bmatrix} K_{11} & K_{12} & 0 & 0 & 0 \\ K_{21} & K_{22} & 0 & 0 & 0 \\ 0 & 0 & K_{33} & K_{34} & K_{35} \\ 0 & 0 & K_{43} & K_{44} & K_{45} \\ 0 & 0 & K_{53} & K_{54} & K_{55} \end{bmatrix}}_{Matrix \ K} \begin{Bmatrix} U_{mn} \\ V_{mn} \\ W_{mn} \\ P_{mn} \\ Q_{mn} \end{Bmatrix} = \begin{Bmatrix} 0 \\ 0 \\ 0 \\ 0 \\ 0 \end{Bmatrix}, \tag{16}$$

for which, the components of matrix  $K$  have been mentioned in Appendix A.

### 6. Numerical results

In this section, effects of various parameters such as weight percentage of single walled carbon nanotube (SWCNT), size effect, fibers orientation, aspect ratio, and thickness on the vibration characteristics of microplates are discussed in details. The values of the different parameters in this study were obtained according to Rafiee et al. [19].

Figure 3 shows the weight percentage effect of SWCNT on dimensionless frequencies versus aspect ratio ( $a/b$ ) of multiscale composite microplates. As can be seen, increasing aspect ratio of microplate leads to increase dimensionless frequencies of microplate.

Also, increasing weight percentage of SWCNT leads to increase stiffness of microplate and consequently leads to improved dimensionless frequencies.

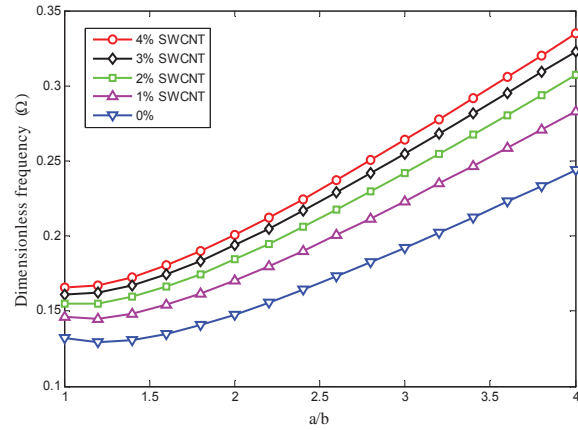


Fig. 3. The weight percentage effect of SWCNT on dimensionless frequencies versus aspect ratio of microplate

Figure 4 illustrates the dimensionless natural frequency versus aspect ratio of microplate in various aspect ratios (length-to-diameter) of CNTs. It can be found that increasing length-to-diameter ratio of CNTs causes the increase of dimensionless frequencies and it is because of the fact that internal structure of microplate are further strengthened. Dimensionless natural frequencies versus length-to-thickness ratio of microplate in various weight percentages of CNTs are studied and depicted in Figure 5. According to this figure, dimensionless frequencies of microplate are reduced by increasing length-to-thickness ratio ( $a/h$ ) of microplate. It is obvious that a higher length-to-thickness ratio which is related to thinner microplate has a lower stiffness. Moreover, SWCNT reinforced composite microplates indicate better resistance to reduced natural frequencies compared to multi-walled carbon nanotube (MWCNT) reinforced composite microplates.

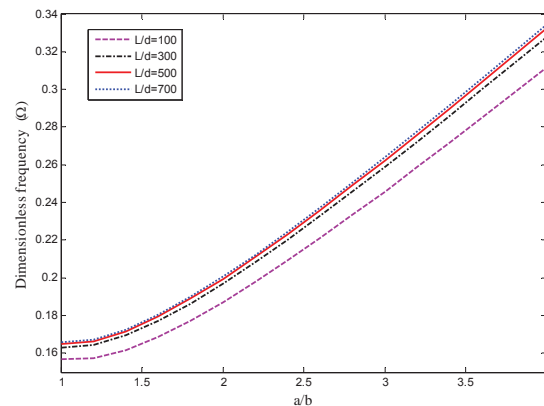


Fig. 4. The influence of SWCNTs aspect ratio on the dimensionless frequencies versus aspect ratio of microplate

Effect of CNT content on the dimensionless natural frequency under various fibers orientation is presented in Figure 6. Increasing volume fraction of CNT, dimensionless natural frequency decreases from 0 to  $\pi/4$  radian and it increases from  $\pi/4$  to  $\pi/2$  radian. Therefore, the results of this figure can help in selecting an appropriate combination of volume fraction of CNT and fibers orientation in order to optimize the design of multiscale composite microplates.

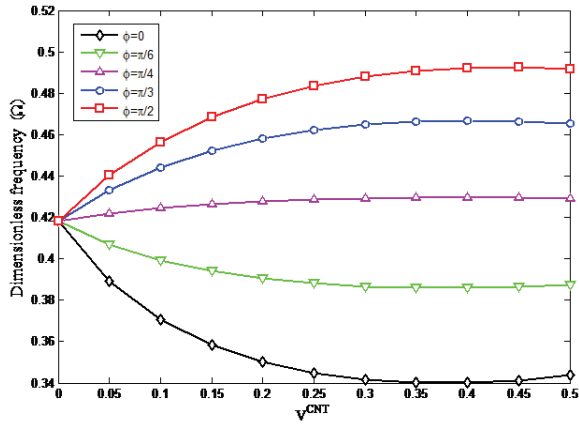


Fig. 5. Dimensionless natural frequency versus length-to-thickness ratio of microplate in various weight percentages of CNTs

Figure 7 shows the size effect on dimensionless natural frequencies in various aspect ratios of microplate. According to this, the results of MCST are as the same of CPT when the material lengths scale parameter is equal to zero. Also, MCST gives the higher natural frequencies respect to CPT. In addition, selecting a higher material lengths scale parameter causes increased dimensionless frequencies, approximately.

In order to verify the reliability of the results, the comparison between the frequencies of isotropic microplate in the present study and the work which is done by Ke et al. [20] is performed. As can be seen in Figure 8, there is a good agreement between the results of present study and the work done by Ke et al. [20].

## 7. Conclusion

This paper develops the vibration analysis of CNTs/fiber/polymer multiscale composite microplates using MCST for the first time. To determine the material properties of the multiscale composite plate, Halpin-Tsai model and fiber micromechanics approach are employed. The motion equations for microplate are derived using FSDT and solved by means of Navier solution for simply supported

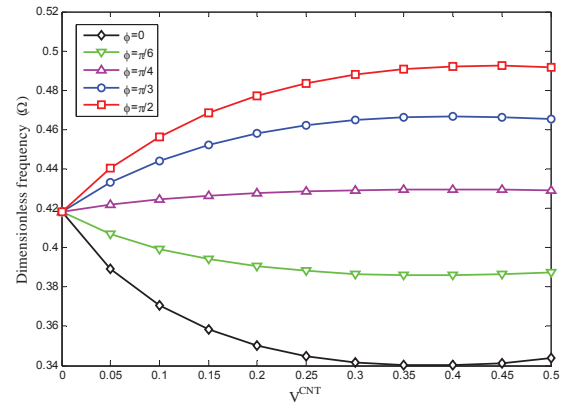


Fig. 6. Effect of CNT content on the dimensionless natural frequency under various fibers orientation

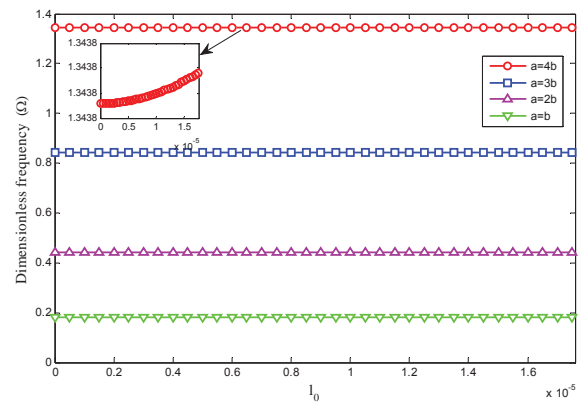


Fig. 7. The size effect on dimensionless natural frequencies in various aspect ratio of microplate

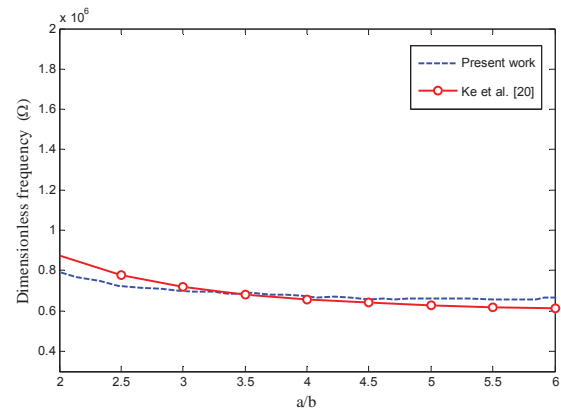


Fig. 8. Comparison between the frequencies of isotropic microplate in the present study and the work which is done by Ke et al. [20]

the weight percentage of SWCNT, size effect, fibers orientation, aspect ratio, and thickness on the vibration characteristics of multiscale composite microplate. It is found that:

- Dimensionless frequencies of microplates are increased by increasing weight percentage of

SWCNT, aspect ratio of microplate, and length-to-diameter ratio of CNTs.

- Dimensionless frequencies of microplate are reduced by increasing length-to-thickness ratio of microplates.
- Increase in the frequencies is more pronounced in the case of microplates reinforced with SWCNT compared with MWCNT.
- The variation of fibers orientation up to  $\pi/4$  radian leads to decrease in dimensionless natural frequency. The variation of fibers orientation more than  $\pi/4$  radian leads to increase in dimensionless natural frequency.
- MCST desires CPT while the material length scale parameter is equal to zero. Also, MCST gives the higher natural frequencies respect to CPT.

### 8. Appendix

The components of matrix  $K$  can be obtained as follows:

$$K_{11} = I_0 \overline{Q}_{11} \alpha^3 K_1 + I_0 \overline{Q}_{66} \alpha K_1 \beta^2 + \frac{1}{16} I_0 M \alpha^3 K_1 \beta^2 + \frac{1}{16} I_0 M \alpha K_1 \beta^4 + I_0 \rho^c \alpha K_1 i^2 \omega^2, \quad (A1)$$

$$K_{12} = -\frac{1}{16} I_0 M \alpha K_1 \beta^4 + I_0 \overline{Q}_{66} \alpha K_1 \beta^2 + I_0 \overline{Q}_{26} \beta^3 K_2 + \frac{1}{16} I_0 M \alpha^3 K_1 \beta^2 + I_0 \overline{Q}_{16} \beta^2 K_1 \alpha + I_0 \overline{Q}_{16} \beta K_2 \alpha^2, \quad (A2)$$

$$K_{21} = -\frac{1}{16} I_0 M \alpha^2 K_3 \beta^3 + I_0 \overline{Q}_{66} \alpha^2 K_3 \beta + I_0 \overline{Q}_{26} \alpha K_2 \beta + \frac{1}{16} I_0 M \alpha^4 K_3 \beta + I_0 \overline{Q}_{16} \alpha^2 K_3 \beta + I_0 \overline{Q}_{16} \alpha^3 K_2, \quad (A3)$$

$$K_{22} = 2I_0 \overline{Q}_{26} \alpha K_2 \beta^2 + I_0 \overline{Q}_{22} \beta^3 K_3 + I_0 \overline{Q}_{66} \alpha^2 K_3 \beta + \frac{1}{16} I_0 M \alpha^4 K_3 \beta + \frac{1}{16} I_0 M \alpha^2 K_3 \beta^3 + I_0 \rho^c \beta K_3 i^2 \omega^2, \quad (A4)$$

$$K_{33} = \rho^c I_2 \alpha^2 K_4 i^2 \omega^2 + \rho^c I_2 \beta^2 K_4 i^2 \omega^2 + I_0 \rho^c K_4 i^2 \omega^2 + \frac{3}{2} I_0 M \alpha^2 K_4 \beta^2 + 2\overline{Q}_{12} I_2 \alpha^2 K_4 \beta^2 + 4\overline{Q}_{66} I_2 \alpha^2 K_4 \beta^2 - 4\overline{Q}_{26} I_2 \alpha K_2 \beta^3 - 4\overline{Q}_{16} I_2 \alpha^3 K_2 \beta + \overline{Q}_{11} I_2 \alpha^4 K_4 + \frac{1}{4} I_0 M \alpha^4 K_4 + \frac{1}{4} I_0 M \beta^4 K_4 + \overline{Q}_{22} I_2 \beta^4 K_4, \quad (A5)$$

$$K_{34} = -\frac{3}{8} I_0 M \alpha^2 K_4 \beta^2 - \rho^c I_2 \alpha^2 K_4 i^2 \omega^2 + 3\overline{Q}_{16} I_2 \alpha^3 K_4 \overline{Q}_{11} I_2 \alpha^4 K_4 - \frac{1}{8} I_0 M \alpha^4 K_4 - \overline{Q}_{12} I_2 \alpha^2 K_4 \beta^2 - 2\overline{Q}_{66} I_2 \alpha^2 K_4 \beta^2 + \overline{Q}_{26} I_2 \alpha K_2 \beta^3, \quad (A6)$$

$$K_{35} = -\frac{3}{8} I_0 M \alpha^2 K_4 \beta^2 + \overline{Q}_{16} I_2 \alpha^3 K_2 \beta - \rho^c I_2 \beta^2 K_4 i^2 \omega^2 + \frac{1}{8} I_0 M \beta^4 K_4 - \overline{Q}_{22} I_2 \beta^4 K_4 - \overline{Q}_{12} I_2 \alpha^2 K_4 \beta^2 + 3\overline{Q}_{26} I_2 \alpha K_2 \beta^3 - 2\overline{Q}_{66} I_2 \alpha^2 K_4 \beta^2, \quad (A7)$$

$$K_{43} = -\rho^c I_2 \alpha K_1 i^2 \omega^2 - 3\overline{Q}_{16} I_2 \alpha^2 K_2 \beta - \frac{3}{8} I_0 M \alpha K_1 \beta + \frac{1}{8} I_0 M \alpha^3 K_1 - \overline{Q}_{26} I_2 \beta^3 K_2 - 2\overline{Q}_{66} I_2 \alpha K_1 \beta^2 - \overline{Q}_{11} I_2 \alpha^3 K_1 - \overline{Q}_{12} I_2 \beta^2 K_1 \alpha, \quad (A8)$$

$$K_{44} = I_0 k_s \overline{Q}_{55} \alpha K_1 + \overline{Q}_{66} I_2 \alpha K_1 \beta^2 + 2\overline{Q}_{16} I_2 \alpha^2 K_2 \beta + \frac{1}{16} M I_2 \alpha^3 K_1 \beta^2 + \frac{1}{2} I_0 M \alpha K_1 \beta^2 + \frac{1}{16} I_0 M \alpha^3 K_1 + \frac{1}{16} M I_2 \alpha K_1 \beta^4 + \rho^c I_2 \alpha K_1 i^2 \omega^2 + \overline{Q}_{11} I_2 \alpha^3 K_1, \quad (A9)$$

$$K_{45} = \overline{Q}_{16} I_2 \alpha^2 K_2 \beta + \overline{Q}_{12} I_2 \beta^2 K_1 \alpha + \overline{Q}_{66} I_2 \alpha K_1 \beta^2 + \overline{Q}_{26} I_2 \beta^3 K_2 - \frac{1}{16} M I_2 \alpha^3 K_1 \beta^2 - \frac{1}{16} M I_2 \alpha K_1 \beta^4 - \frac{5}{16} I_0 M \alpha K_1 \beta^2, \quad (A10)$$

$$K_{53} = -\frac{1}{8} I_0 M \beta^3 K_3 - \rho^c I_2 \beta K_3 i^2 \omega^2 - 2\overline{Q}_{66} I_2 \alpha^2 K_3 \beta + \overline{Q}_{16} I_2 \alpha^3 K_2 - \overline{Q}_{22} I_2 \beta^3 K_3 - 3\overline{Q}_{26} I_2 \alpha K_2 \beta^2 - \frac{3}{8} I_0 M \alpha^2 K_3 \beta - \overline{Q}_{12} I_2 \alpha^2 K_3 \beta, \quad (A11)$$

$$K_{54} = \overline{Q}_{66} I_2 \alpha^2 K_3 \beta - \frac{5}{16} I_0 M \alpha^2 K_3 \beta + \overline{Q}_{26} I_2 \alpha K_2 \beta^2 + \overline{Q}_{16} I_2 \alpha^3 K_2 + \overline{Q}_{12} I_2 \alpha^2 K_3 \beta - \frac{1}{16} M I_2 \alpha^4 K_3 \beta - \frac{1}{16} M I_2 \alpha^2 K_3 \beta^3, \quad (A12)$$

$$K_{55} = I_0 k_s \overline{Q}_{44} \beta K_3 + \frac{1}{2} I_0 M \alpha^2 K_3 \beta + 2\overline{Q}_{26} I_2 \alpha K_2 \beta^2 + \rho^c I_2 \beta K_3 i^2 \omega^2 + \overline{Q}_{66} I_2 \alpha^2 K_3 \beta + \overline{Q}_{22} I_2 \beta^3 K_3 + \frac{1}{16} M I_2 \alpha^2 K_3 \beta^3 + \frac{1}{16} M I_2 \alpha^4 K_3 \beta + \frac{1}{16} I_0 M \beta^3 K_3, \quad (A13)$$

where

$$\begin{aligned}
 K_1 &= \int_0^b \int_0^a (\cos(\alpha x) \sin(\beta y)) (\cos(\alpha x) \sin(\beta y)) dx dy, \\
 K_2 &= \int_0^b \int_0^a (\sin(\alpha x) \cos(\beta y)) (\cos(\alpha x) \sin(\beta y)) dx dy, \quad (A14) \\
 K_3 &= \int_0^b \int_0^a (\sin(\alpha x) \cos(\beta y)) (\sin(\alpha x) \cos(\beta y)) dx dy, \\
 K_4 &= \int_0^b \int_0^a (\sin(\alpha x) \sin(\beta y)) (\sin(\alpha x) \sin(\beta y)) dx dy.
 \end{aligned}$$

## References:

- [1] Fleck, N.A., Muller, G.M., Ashby, M.F. and Hutchinson J.W. (1994). Strain gradient plasticity: theory and experiment, *Acta Metallurgica et Materialia*, **42**(2): 475–487.
- [2] Stolken, J.S. and Evans, A.G. (1998). A microbend test method for measuring the plasticity length scale, *Acta Materialia*, **46**(14): 5109–5115.
- [3] Chong, A.C.M., Yang, F., Lam, D.C.C. and Tong, P. (2001). Torsion and bending of micron-scaled structures, *Journal of Materials Research*, **16**(4): 1052–1058.
- [4] Koiter, W.T. (1964). Couple stresses in the theory of elasticity, I and II, *Proceedings of the Koninklijke Nederlandse Akademie van Wetenschappen, Series, B* **67**: 17–44.
- [5] Eringen, A.C. (1972)., Nonlocal polar elastic continua, [International Journal of Engineering Science](#) **10**(1): 1–16.
- [6] Lam, D.C.C., Yang, F., Chong, A.C.M., Wang, J. and Tong, P. (2003). Experiments and theory in strain gradient elasticity, *Journal of the Mechanics and Physics of Solids*, **51**(8): 1477–1508.
- [7] Yang, F., Chong, A.C.M., Lam, D.C.C. and Tong, P. (2002). Couple stress based strain gradient theory for elasticity, *International Journal of Solids and Structures*, **39**(10): 2731–2743.
- [8] Tsiatas G.C. (2009). A new Kirchhoff plate model based on a modified couple stress theory, *International Journal of Solids and Structures*, **46**(13): 2757–2764.
- [9] Yin, L., Qian, Q., Wang, L. and Xia, W. (2010). Vibration analysis of microscale plates based on modified couple stress theory, *Acta Mechanica Solida Sinica*, **23**(5): 386–393.
- [10] Jomehzadeh, E., Noori, H.R. and Saidi, A.R. (2011). The size-dependent vibration analysis of micro plates based on a modified couple stress theory, *Physica E: Low-dimensional Systems and Nanostructures*, **43**(4), 877–883.
- [11] Asghari, M. (2012). Geometrically nonlinear micro-plate formulation based on the modified couple stress theory, *International Journal of Engineering Science*, **51**: 292–309.
- [12] Sahmani, S. and Ansari, R. (2013). On the free vibration response of functionally graded higher-order shear deformable microplates based on the strain gradient elasticity theory, *Composite Structures*, **95**: 430–442.
- [13] Mohammadimehr, M., Mohandes, M. and Moradi, M. (2014). Size dependent effect on the buckling and vibration analysis of double bonded nanocomposite piezoelectric plate reinforced by BNNT based on modified couple stress theory, *Journal of Vibration and Control*, doi: 10.1177/1077546314544513.
- [14] Kim, M., Park, Y.B., Okoli, O.I. and Zhang, C. (2009). Processing, characterization, and modeling of carbon nanotube-reinforced multiscale composites, *Composites Science and Technology*, **69**(3-4): 335-342.
- [15] Bhardwaj, G., Upadhyay, A.K., Pandey, R. and Shukla, K.K. (2013). Non-linear flexural and dynamic response of CNT reinforced laminated composite plates, *Composites Part B: Engineering*, **45**(1): 89-100.
- [16] Reddy, J.N. (2004). *Mechanics of Laminated Composite Plates and Shells: Theory and Analysis*, CRC Press, Boca Raton, FL, Second Edition.
- [17] GhorbanpourArani, A. and Haghparast, E. (2015). Size-dependent vibration of axially moving viscoelastic microplates based on sinusoidal shear deformation theory, *International Journal of Applied Mechanics*.
- [18] Ghorbanpour Arani, A., Khoddami Maraghi, Z. and Khani Arani, H. (2015). Orthotropic patterns of Pasternak foundation in smart vibration analysis of magnetostrictive nanoplate, *Journal of Mechanical Engineering Science*, doi: 10.1177/0954406215579929.
- [19] Rafiee, M., He, X.Q., Mareishi, S. and Liew, K.M. (2014). Modeling and stress analysis of smart CNTs/fiber/polymer multiscale composite plates, *International Journal of Applied Mechanics*, **6**(3): 1450025-1450048.
- [20] Ke, LL., Wang, Y.S., Yang, J. and Kitipornchai, S. (2012). Free vibration of size-dependent Mindlin microplates based on the modified couple stress theory, *Journal of Sound and Vibration*, **331**: 94–106